Genomics 106 (2015) 96–106

Contents lists available at ScienceDirect

Genomics

journal homepage: www.elsevier.com/locate/ygeno

Personalized diagnosis of medulloblastoma subtypes across patients and model systems

Deena Mohamad Ameen Gendoo [a,b,*], Petr Smirnov [a], Mathieu Lupien [a,b,c], Benjamin Haibe-Kains [a,b,*]

[a] Bioinformatics and Computational Genomics Laboratory, Princess Margaret Cancer Center, University Health Network, Toronto, Ontario, Canada
[b] Medical Biophysics Department, University of Toronto, Toronto, Ontario, Canada
[c] Ontario Institute for Cancer Research, Toronto, Ontario M5G 1L7, Canada

ARTICLE INFO

Article history:
Received 4 May 2015
Accepted 6 May 2015
Available online 12 May 2015

Keywords:
Cancer
Medulloblastoma
Classification
Subtypes
Human
Mouse model

ABSTRACT

Molecular subtyping is instrumental towards selection of model systems for fundamental research in tumor pathogenesis, and clinical patient assessment. Medulloblastoma (MB) is a highly heterogeneous, malignant brain tumor that is the most common cause of cancer-related deaths in children. Current MB classification schemes require large sample sizes, and standard reference samples, for subtype predictions. Such approaches are impractical in clinical settings with limited tumor biopsies, and unsuitable for model system predictions where standard reference samples are unavailable. Our developed *Medullo-Model To Subtype* (MM2S) classifier stratifies single MB gene expression profiles without reference samples or replicates. Our pathway-centric approach facilitates subtype predictions of patient samples, and model systems including cell lines and mouse models. MM2S demonstrates >96% accuracy for patients of well-characterized normal cerebellum, WNT, or SHH subtypes, and the less-characterized Group 4 (86%) and Group 3 (78.2%). MM2S also enables classification of MB cell lines and mouse models into their human counterparts.

1. Introduction

Medulloblastoma (MB) subtype stratification has evolved with the increased availability of genomic data and improved understanding of MB inter-tumor heterogeneity, signalling pathways, and molecular pathogenesis mechanisms [1–5]. Four MB subtypes, referred to as the WNT, SHH, Group 3, and Group 4, are recognized. These differ based on histopathology, epidemiology, prognosis, and genomic profiles [4,5]. Of these, Group 3 and Group 4 exhibit poor prognosis and are poorly characterized at the molecular level, thus presenting ongoing clinical challenges [1–7]. Ongoing studies to determine subtype-specific biological mechanisms currently involve extensive gene expression profiling and sequencing of MB subtypes, to detect recurrent mutations, novel SNVs, CNAs, and CpG methylation sites [7–9]. These efforts were instrumental to improving MB subtype classification but relied on large data sets, a requirement not easily attainable in future classification studies where limited sample sizes are available. This concern instigated development of several MB prediction assays in a clinical setting [4,10,11]. These include identification of a set of 22 subtype-specific signature genes using nanoString nCounter technology to measure mRNA expression from FFPE [11], as well as development of a 13-gene multiplex mRNA expression signature specific for the WNT and SHH subtypes [10]. Unfortunately, these signatures have not been further developed into automated classifiers for use by researchers and clinicians. To use these signatures, new MB samples would need to be interrogated by hierarchical cluster analysis or other orthogonal methods, which requires additional external samples to generate comparisons. Accordingly, the proposed classification practices have provided a systems-wide view of subtype tumorigenesis, but remain deficient in providing individualized predictions of particular MB samples.

The need for personalized predictors of MB samples is not only necessary for prediction of patient samples, but also for predictions of samples pertaining to model systems. These latter predictions are important for future research that utilizes MB cell lines and mouse models to study MB subtype disease origins and signaling pathways [12]. Applicability of current classification schemes towards model predictions is unclear, especially as the reference 'gold standard' to compare model systems to human subtypes remains highly ambiguous. The developed Agreement of Differential Expression (AGDEX) algorithm attempted to address this problem by comparing expression of orthologous genes to determine transcriptomic similarities between tissues from different experiments [13–15]. However, AGDEX relies on *a priori* assumptions regarding

Abbreviations: MB, medulloblastoma; MM2S, Medullo-Model To Subtype; MH2H, medullo-human to human; MM2H, medullo-mouse to human; IHC, immunohistochemistry; FFPE, formalin-fixed paraffin embedded; GTML, Glt1-tTA (glutamate transporter 1-tetracycline transactivator) and tetracycline response element (TRE)-MYCN/luciferase (Luc) mouse medulloblastoma; MCC, Matthews correlation coefficient; GEO, Gene Expression Omnibus; KNN, *k*-nearest neighbor; PCA, principal component analysis.

* Corresponding authors at: Princess Margaret Cancer Centre, University Health Network, Toronto, Ontario, Canada.
E-mail addresses: deena.gendoo@utoronto.ca (D.M.A. Gendoo), bhaibeka@uhnresearch.ca (B. Haibe-Kains).

http://dx.doi.org/10.1016/j.ygeno.2015.05.002
0888-7543/

which samples can be compared in subtype differential expression analyses, which introduces user bias and ultimately prevents robust classification of single tumor samples. Additionally, the algorithm also necessitates a user-selected reference model, perhaps human or mouse normal cerebellum, to generate differential analysis comparisons. Any *a priori* assumptions of reference samples may yield imprecise comparisons with the tested data sets and is doubly problematic when matched reference samples to the tested data are unavailable.

Collectively, current classification methods remain impractical for both research and clinical settings, where reference samples are unattainable, or limited samples or tumor materials are available. They fail to address the critical requirement of generating *personalized, single-sample* predictions for both MB patients and samples pertaining to model systems. To address this focal and much-needed research direction in MB, we developed a novel, *Medullo-Model To Subtype* (MM2S) classifier that matches individual MB samples against human medulloblastoma subtypes. To the best of our knowledge, MM2S is the first *single-sample* classifier of MB samples, which does not rely on a reference sample or multiple sample replicates to generate predictions. We developed a systems-based methodology that facilitates application of the MM2S algorithm to MB subtype prediction of both patient samples and model systems, including cell lines and mouse models. We demonstrate the efficacy and versatility of MM2S via the largest MB stratification analysis of 23 publicly gene expression data sets, spanning 754 patients, 26 cell lines, and 261 mouse samples. We discuss the implications of MM2S towards narrowing the gap between MB subtype classification methods and the development of singular, subtype-specific diagnosis of patients, cell lines, and mouse models.

2. Results

2.1. MM2S accuracy on human medulloblastoma training samples

We trained the MM2S classifier on the 347 human samples from three data sets and pre-validated its accuracy in correctly predicting

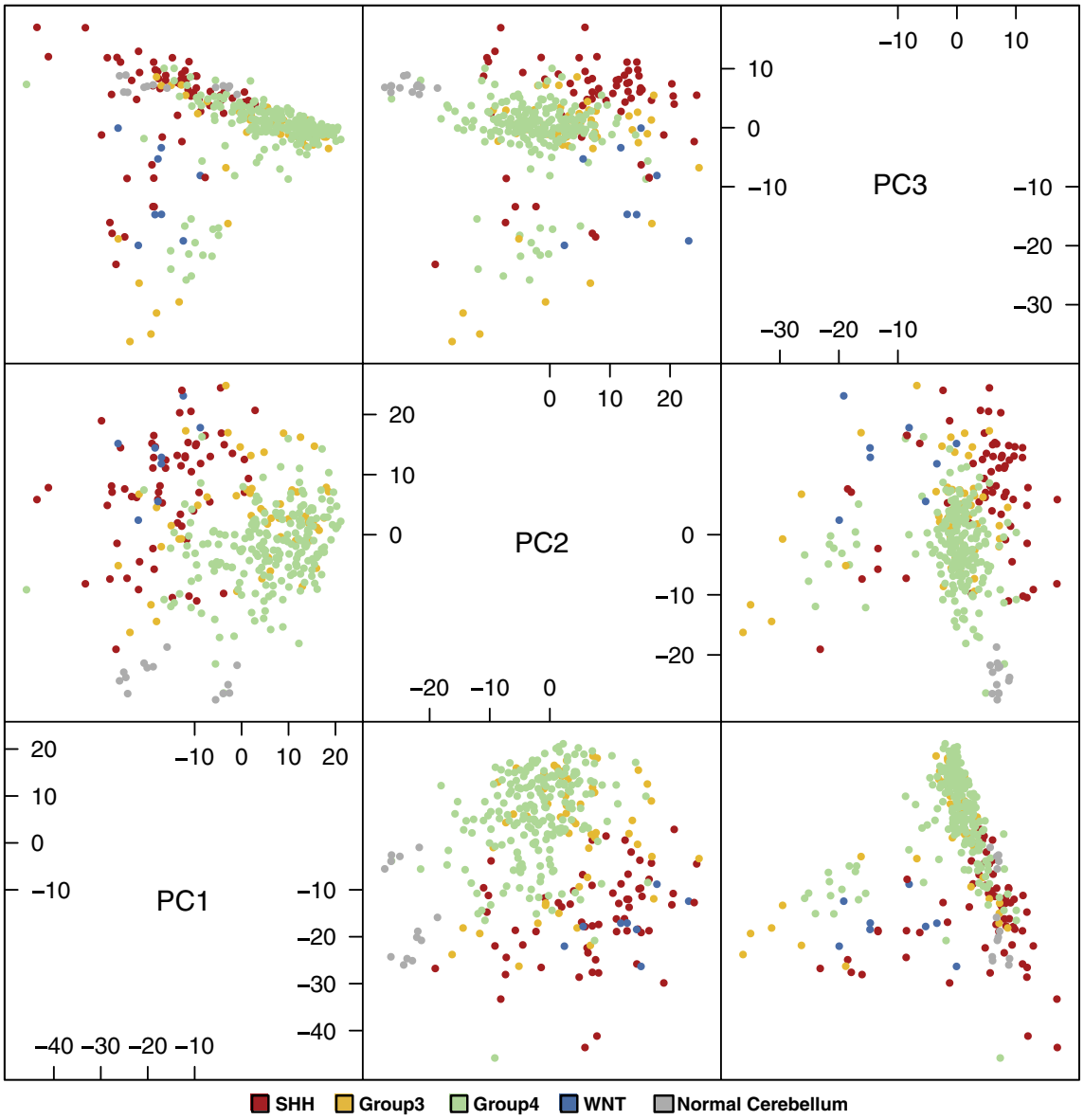

Fig. 1. Principal component analysis of 674 ssGSEA-ranked gene sets (rank matrix) for the human training data set. This is a principal component analysis (PCA) of the human training set, prior to feature selection. Shown is a lattice plot of the first three principal components, with principal components axes rendered across the diagonal. PC1-PC2, PC1-PC3, and PC2-PC3 represent the three plots above the diagonal and are mirrored in the three plots below the diagonal. Samples are colored by subtype.

human MB subtypes before testing it on independent human and mouse samples. A pathway activity matrix of these samples, prior to selection of MM2S hyperparameters, indicates strong clustering of subtype-specific samples across the three data sets [Fig. 1]. To tune the hyperparameters of the MM2S classifier, we performed multiple 10-fold cross-validation on the training set, repeated 100 times. We observed that the best model was obtained by selecting the $k = 5$ nearest neighbors in a genomic space defined by 104 unique gene sets [S1: Table S1(A)], which were used to generate a ranked matrix of pathway activity scores (see Methods). In this setting, the classifier was able to correctly classify human samples with high levels of accuracy for normal cerebellum (100%) and well-studied MB groups such as SHH (100%) and WNT (100%), as well as the less characterized Group 4 (97.6%) and Group 3 (66.6%) subtypes [S2: Table S2]. Despite the imbalance of the subtypes in this training data set, with Group 4 constituting the largest group and WNT samples constituting the smallest, we did not observe strong biases toward Group 4 subtype class predictions.

2.2. MM2S prediction of MB subtypes on human samples

We tested MM2S prediction effectiveness on independent human samples generated on a variety of microarray platforms, spanning 407 MB samples across four separate data sets [Fig. 2A, S3: Table S3(A–E), S4: Table S4(A–D)]. Despite the difference in subtype sample sizes across these data sets, MM2S predictions remain robust for the well-studied WNT and SHH subtypes, as well as normal cerebellum, exhibiting 96–100% accuracy across the data sets [Fig. 2B]. All the samples pertaining to WNT group and normal cerebellum in the respective data sets predict correctly [Fig. 2A], despite that these groups represents the smallest groups within the MM2S training set. Group 3 and Group 4 prediction accuracy ranges between 74% and 87% for most data sets. A substantial proportion of Group 3 samples are misclassified as Group 4, which may reflect upon weak molecular characterization of these subtypes [Fig. 2A]. However, we observed that the prognostic value of our classifier is statistically similar to the published classification of MB samples across these groups [Fig. 3], thereby underscoring the validity of the subtypes. Accordingly, the observed concordance between original and MM2S classifications supports the biomedical relevance of the classifier. The combined MM2S prediction accuracy for each subtype is reported in Table S3(E). We also applied our classifier to the limited number of human MB cell lines publicly available [S4: Table S4(O)] and note that the majority of cell line predictions belong to either WNT or SHH, but not Group 3 or Group 4.

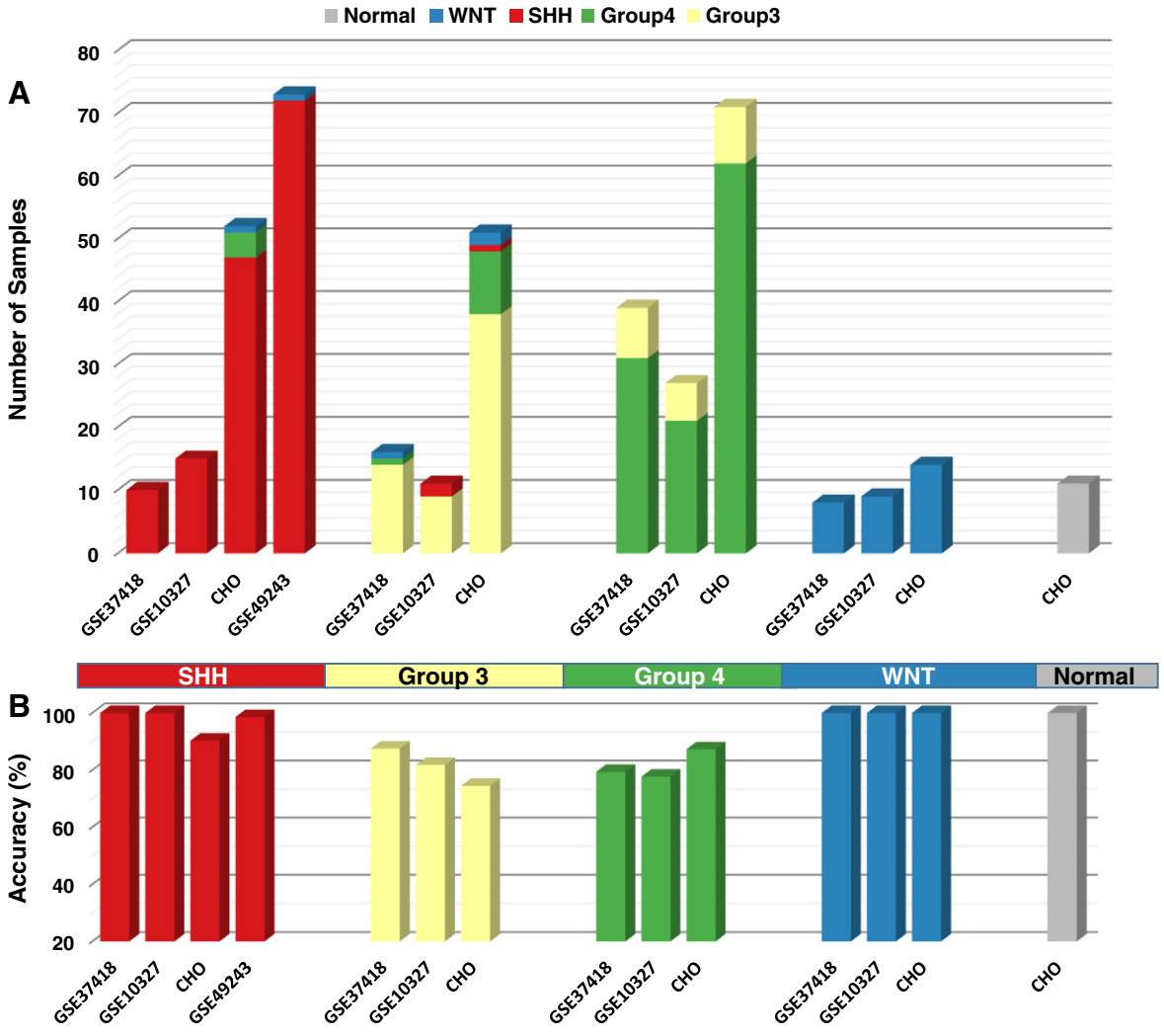

Fig. 2. Overall sample predictions and subtype-specific accuracy of MM2S predictions across four human patient data sets. Data sets are clustered together by subtype (depicted by the central bar). (A) A stacked bar plot indicates overall samples predictions across the subtypes. Each bar represents a data set, with the height of the bar indicating the number of subtype-specific samples pertaining to that data set. Columns are colored to represent the number of predictions across the subtype that have been correctly predicted by MM2S, as well as misclassified samples. (B) The prediction accuracy of MM2S, for each subtype, across the four data sets.

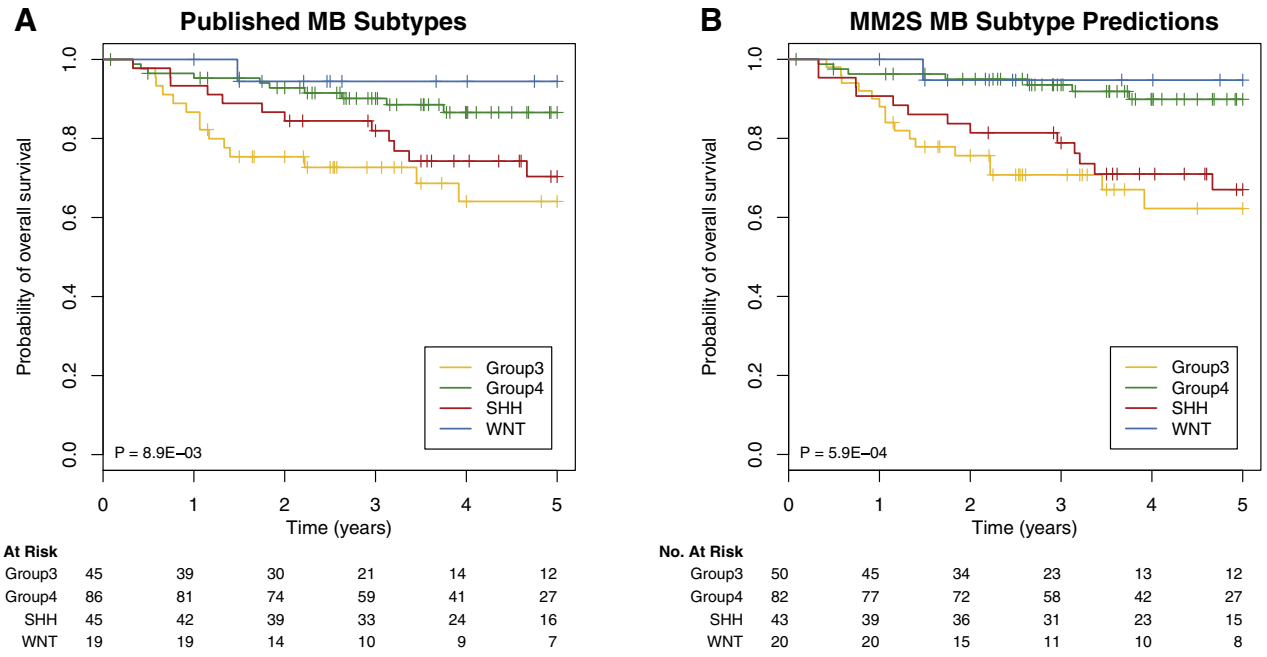

Fig. 3. Survival curves of MB patients with respect to subtypes. (A) Kaplan–Meir survival curves censored at 5 years for patients based on their original MB subtype classification. (B) Kaplan–Meir survival curves censored at 5 years for the same patients in (A), based on MM2S subtype predictions. The statistically significant prognositic value of both classifications are presented (log-rank $p < 0.001$).

2.3. MM2S prediction of MB subtypes on mouse samples

To demonstrate MM2S flexibility and applicability for cross-species prediction of MB subtypes, we used our algorithm in a meta-analysis of 261 murine samples across 10 data sets to classify the mouse MB models into their human counterparts [Table 1, S4: Table S4(E–N)]. For each data set, calculations were based on a ranked matrix of activity scores of unique and subtype-discriminative gene sets [S1: Table S1(F–Q)] between the human and mouse data sets.

MM2S facilitate subtype predictions across for single mouse samples, as well as establishing a consensus prediction across replicates of a mouse models. Our tested data set spans at least 20 mouse models [Table 1], in addition to normal cerebellum. We focus here on mouse models that are heavily used in *in vivo* MB studies and demonstrate overall MM2S predictions across all the replicates of these models [Fig. 4, Table 1]. MM2S demonstrates relative consistency of subtype predictions across replicates of well-studied mouse models. Ptch-mutated mouse models [16] (Ptch$^{+/-}$, Math1-creERT2::Ptch1$^{Fl/Fl}$, Nestin-creERT2::Ptch1$^{Fl/Fl}$, Ptch1$^{+/-}$Cdkn2C$^{-/-}$), which are experimentally associated with the SHH subtype, all predict as SHH across several data sets [Fig. 4]. Consensus predictions of experimentally associated SHH mouse models such as SmoM2 (Math1-cre::SmoM2$^{Fl/+}$, hGFAP-cre::SmoM2$^{Fl/+}$) [16] also predict by MM2S as belonging to SHH subtype [Fig. 4]. We compared how our MM2S algorithm compares against existing subtype classifications algorithms, including the agreement of differential expression (AGDEX) analysis for each of mouse models. There is a strong concordance between MM2S and AGDEX across murine models that are predicted as SHH, as well as the Group 3 GTML model [Fig. 4]. Distinctively, the presence of a normal subtype, and the subsequent prediction of normal cerebellum samples, is a new addition in MM2S that is unavailable in AGDEX. More than 80% of the normal cerebellum samples tested MM2S correctly predict as normal, with the exception of a small number of samples that predict as SHH. These "tumor-like" samples may reflect upon sample heterogeneity and/or technical variation (e.g., experimental processing) in the samples that distinguishes them from true normal mouse cerebellum. Interestingly, all of the mispredicting samples were biological replicates of normal P7 cerebellum and pertained to the same data set (GSE36594).

The ability of MM2S to conduct singular sample predictions facilitates further investigation into tumor heterogeneity and the exploration of potential intermediate phenotypes. The simplicity of our approach facilitates the identification of the first- and second-choice human subtypes for each sample replicate of a particular mouse model [Fig. 5A]. This is in stark contrast to AGDEX, where a summarized AGDEX score is produced across all replicates of the model. Using our personalized prediction scores, we investigated the distribution of subtype predictions across all replicates of the GTML mouse model (Glt1-tTA (glutamate transporter 1-tetracycline transactivator) and tetracycline response element (TRE)-MYCN/luciferase (Luc) mouse medulloblastoma) [Fig. 5B]. This was the only mouse model for which we have observed Group 3 predictions across a large number of sample replicates, suggesting the potential for a non-SHH mouse model. There are 32 sample replicates for this model, 20 of which predict as Group 3, many with high degree of confidence (>80%) [Fig. 5B]. Based on these predictions, the GTML mouse model shown can be confidently labeled by a majority consensus as a Group 3 medulloblastoma model. However, there are a number of samples that predict as SHH and a small subset of "normal-like" tumor samples [Fig. 4, Fig. 5B], suggesting that further investigation would need to be conducted on these heterogeneous samples to assess their validity for use as a Group 3 mouse model.

The use of single-sample classifications opens a new research avenue into potential intermediate phenotypes. We investigated sample predictions of the WNT-associated Blbp-cre::Ctnnb1(ex3)$^{Fl/+}$ Trp53$^{Fl/Fl}$ mouse model, which produced conflicting predictions with MM2S compared to AGDEX [Fig. 4, Fig. 5C]. Using MM2S, half of the samples predict as WNT and other half as SHH. The conflicting predictions we have observed may reflect upon a heterogeneous, intermediate, murine model. Previous classification of this model using AGDEX indicated that the second-highest and significantly predicting group for this model, following WNT, is SHH [15]. Whether this model represents a heterogeneous

Table 1
Confusion matrix of human MB subtype predictions for 10 mouse testing sets. The major mouse models represented in each data set are highlighted, as well as the total number MB subtype predictions across the data set.

Moue datasets		Predicted medulloblastoma subtypes using MM2S				
Dataset	Major mouse models represented	SHH	WNT	Group 3	Group 4	Normal
GSE36594 (n=56)	▪ Normal P7 cerebellum (n=5) ▪ GTML medulloblastoma tumor (n=32) ▪ Orthotopic E16 cerebellar tumor (n=3) ▪ Orthotopic P0 cerebellar tumor (n=3) ▪ Orthotopic P0 forebrain tumor (n=3)	34		20		2
GSE24628 (n=16)	▪ Ctnnb1 MB (n=3) ▪ Ptch1 MB (n=6) ▪ Embryonic dorsal brainstem (n=4) ▪ Postnatal granule neuron precursor cells (n=3)	7	2			7
GSE33199 (n=64)	▪ Shh–type medulloblastoma from [Cdkn2c−/−; Trp53Fl/Fl; Nestin–Cre] and [Cdkn2c−/−; Ptch1+/−] (n=16) ▪ Myc and Mycn overexpression in Cdkn2c−/−, Trp53−/−cerebellar cells (n=42) ▪ Wnt–type medulloblastomas from CTNNB1+/lox (ex3); BLBP–Cre; Trp53Fl/Fl (n=3)	63	1			
GSE11859 (n=27)	▪ Math1–cre: SmoM2 cerebellar tumor (n=3) ▪ Tlx3–cre: SmoM2 cerebellar tumor (n=3) ▪ Olig2–tva–cre: SmoM2 cerebellar tumor (n=7) ▪ hGFAP–cre: SmoM2 cerebellar tumor (n=6) ▪ Ptc1+/–cerebellar tumor (n=2) ▪ Non–tumor cerebellar tissue control (n=6)	18			2	7
GSE50824 (n=19)	▪ Math1+ neuronal progenitors (n=4) ▪ Nestin+ neuronal progenitors (n=4) ▪ Math1–CreERT2/Ptch1C/C mice (n=4) ▪ Nestin–CreERT2/Ptch1C/C mice (n=4) ▪ CD133+, Lin−cerebellar progenitors (n=3)	19				
GSE19534 (n=26)	▪ Cerebellum wild type 6 month (n=3) ▪ Cerebellum SNCA knockout 6 month (n=3) ▪ Striatum wild type 6 month (n=3) ▪ Striatum SNCA knockout 6 month (n=3) ▪ Cerebellum wild type 21 month (n=4) ▪ Cerebellum SNCA knockout 21 month (n=4) ▪ Striatum wild type 21 month (n=3) ▪ Striatum SNCA knockout 21 month (n=3)					26
GSE34126 (n=19)	▪ Normal stem cells (n=5) ▪ Stem cell–derived tumors (n=5) ▪ Patched tumors (n=4) ▪ Progenitor–derived tumors (n=5)	19				
GSE2426 (n=14)	▪ Cerebellar granule cell precursors (GCPs) (n=4) ▪ Preneoplastic cells were obtained from 6 week–old patched mutants (n=5) ▪ Math1–GFP/patched+/–tumour (n=5)	8	1			5
GSE9299_ 430A (n=5)	▪ Wild type cerebellum (n=4) ▪ Medulloblastoma from CAGGS–CreER; R26–SmoM2 mice (n=6)	3				2
GSE9299_ 430B (n=5)		5				
GSE6463_ 430A (n=5)	▪ Granule neuron precursors (n=6) ▪ Granule neuron precursors infected with retroviruses that express N–myc (n=4)	5				
GSE6463_ 430B (n=5)		5				

group remains to be determined with the profiling of additional mouse replicates in future studies.

2.4. The MM2S server

The generation of subtype-specific predictions of medulloblastoma samples is a challenging process that requires substantial computation and data processing to generate predictions. We introduce here the first free, automated, and publicly available web service called MM2S. This service is available at <opennet-33-129.uhnres.utoronto.ca/mm2s/mm2s.html> and only requires normalized gene expression profiles for samples of interest as input. Results that are generated for each of the samples include the final MM2S prediction as well as the neighboring subtype predictions for each sample. We thus provide the user with predictions of the highest ranking and second-highest subtypes that can be attributed to any particular sample [Fig. 5]. This aids in the interpretability of the results for diagnostic characterization of MB samples.

3. Discussion

The development of a flexible subtype classification method for MB is a great challenge and poses an obstacle for stratification of MB patients and model systems. We have developed MM2S, the first single-sample, medulloblastoma-specific classifier that allows for the easy classification of human MB patient samples and model systems to their corresponding human medulloblastoma subtypes. Using our MM2S classifier, we conducted the largest meta-analysis of human patients, cell lines, and mouse MB gene expression data from variable microarray platforms and different sources of origin. We have demonstrated the versatility and robustness of MM2S towards prediction of MB samples across these diverse data sets and MB samples. Our classifier demonstrates statistically significant and similar prognostic value to the current classification of MB human patient tumors, which supports the validity of our predictions.

Our MM2S classifier demonstrates significant novelty over other MB classification schemes by providing *personalized* predictions, without requiring a reference sample (e.g., human cerebellum), or multiple replicates per sample to generate subtype comparisons. This asset makes MM2S versatile for diagnostic classification of patients in basic research and preclinical settings, as well stratification of MB samples that have been generated on different platforms and different model systems. Another innovative feature of MM2S is that "normal" state is considered as a subtype within our classifier. This may serve to identify "normal-like" tumor samples, or conversely, "normal" reference samples that mispredict as tumor subtypes. Such cases may represent instances of human error (mislabeling of samples), technical error (contamination within samples), or even biological variation (undifferentiated and early stage tumor samples). With the ability to identify confidence thresholds for each sample, ambiguous samples can now be discarded or further explored. Undoubtedly, this promises to help minimize assumptions that are made during the classification process, and subsequently aid in accurate assessment of MB samples and their subsequent management.

The above-mentioned features introduced within MM2S are significant additions that have not been observed in previous classification schemes. We have compared our findings against AGDEX, which is to date the only classification method that promoted cross-species predictions of MB samples. MM2S flexibility of predicting mouse models supersedes the AGDEX classification method, where one must combine potential replicates into a particular subtype to conduct differential expression analysis against a reference set of samples. To properly conduct such an analysis, this assumes (i) the existence of a reference genotype such as normal human cerebellum and (ii) the correct assignment of samples to a particular group for transcriptomic comparison against the reference genotype. These requirements have been alleviated under MM2S, which reduces potential sources of bias as well as ambiguity in interpretation of the results.

The MM2S system demonstrates robustness in prediction of human patient samples across a heterogeneous compendium of data sets. MM2S predicts the same human subtypes for sample from each of the four MB subtypes, as well as for normal cerebellum, with high degrees of accuracy. The concordance between our predictions and the original

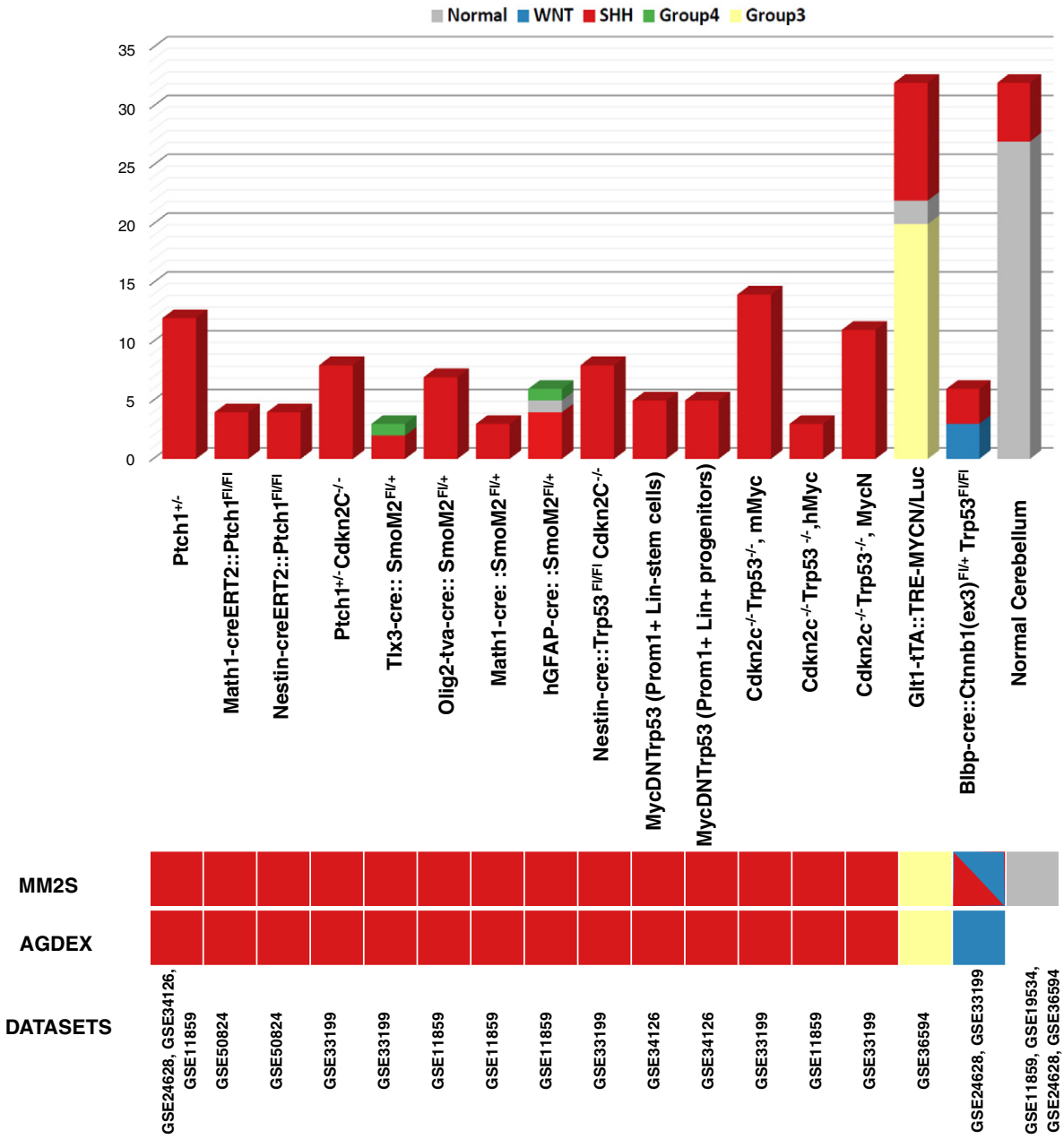

Fig. 4. MM2S sample predictions across 16 murine MB models and normal cerebellum samples. A stacked bar plot (top) indicates overall predictions across all sample replicates of each mouse model. Each bar represents a mouse model, with the height of the bar indicating the corresponding number of replicates. Columns are colored to represent the number of replicates across each model that are predicted by MM2S as pertaining to SHH (red), Group 3 (yellow), Group 4 (green), WNT (blue), or normal (black). The subtype majority prediction for each model is indicated (bottom), as well as comparison of the majority predictions to AGDEX classification of the same model. The murine data sets from which the models have been selected are indicated.

subtype classification is highly pronounced for samples originating from well-characterized subtypes, including SHH and WNT. Despite Group 3 and Group 4 being less characterized at the molecular level, MM2S still succeeds in generating accurate predictions with high degrees of accuracy for Group 4 (83.2%) and Group 3 (78.2%), with similar prognostic value to current MB subtype classifications of these samples [Fig. 2, Fig. 3, Table S3(E)]. The decrease in accuracy of our Group 3 and Group 4 predictions, compared to SHH and WNT, may reflect upon the molecular complexity of these subtypes. Notably, we have demonstrated that the MM2S algorithm can also be extended towards MB predictions of gene expression profiles derived from cell line data sets in addition to primary tumors and mouse models.

The MM2S systems-based algorithm is flexible for use towards cross-species prediction of MB subtypes, such as molecular characterization of MB mouse models. We have demonstrated that MM2S predicts the same human counterparts for several well-studied mouse MB models that were experimentally designed to be associated with a particular human subtype [Fig. 4, Table 1]. This observed computational and experimental concordance may serve, to some extent, as an experimental

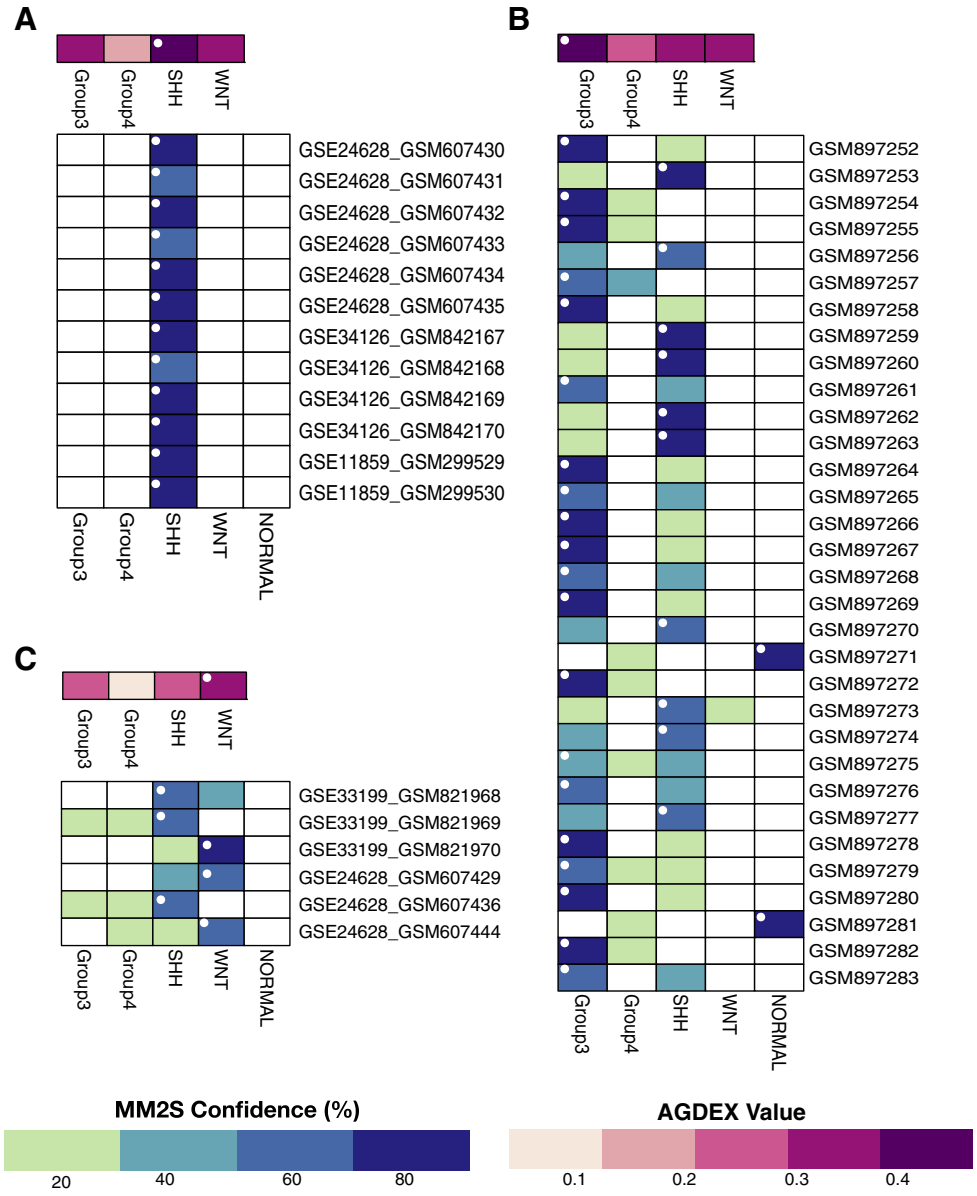

Fig. 5. MM2S sample predictions across a representative SHH, Group 3, and WNT mouse model. A heatmap representation is provided with MM2S confidence intervals across all MB subtypes (including normal), for each sample replicate within a mouse model. A white dot indicates the final subtype selection of a particular sample. The range of AGDEX scores provided for the overall mouse model is also represented. Depicted are three mouse models. (A) Ptch +/−, (B) GMTL mouse model replicates from GSE36594, (C) Blbp-cre::Ctnnb1(ex3)$^{Fl/+}$ Trp53$^{Fl/Fl}$ mouse model. For all replicates of a model, sample names are provided. For models containing samples from multiple data sets (A,C), the corresponding data set is also indicated.

validation of some our predictions. Despite vast differences in our approach, our findings also corroborate with AGDEX for the well-studied mouse models.

Our MM2S investigations on mouse models indicate the potential for future development of non-SHH mouse models. Given the difficulty in identification of non-SHH models [16], this will be a welcome development and a significant advancement for MB research in this area. We have identified a clear example of a Group 3 mouse model (GTML), as well as the existence of a potentially heterogeneous mouse model (Blbp-cre::Ctnnb1(ex3)$^{Fl/+}$ Trp53$^{Fl/Fl}$). We have highlighted that, while our findings are largely corroborated with AGDEX, MM2S supersedes AGDEX by further identifying the exact samples that have driven the overall prediction of these mouse models. In the case of the GTML mouse model for example, MB scientists can now focus on the subset of replicates which exhibit high confidence as Group 3 when conducting future research using these samples. Our personalized approach will be instrumental for future MB research that relies on mouse models to understand MB subtype-specific pathogenesis *in vitro*.

Our study has several potential limitations. First, while MM2S succeeds in generating single-sample, individual classifications, it is important to acknowledge that early pre-processing of these samples prior to classification is not necessarily conducted at the single-sample level. One may argue that a single-sample GSEA, in which the absolute expression of the genes is compared, requires an input of a single-sample normalized gene expression values using standard algorithms such as frozen RMA or MAS5.0, instead of RMA. The MAS5 algorithm is no longer applicable to human or mouse gene ST platforms, and fRMA implementation for the Gene 1.1 ST platforms, which were used in this analysis, is currently lacking. Thus, we opted to use the RMA algorithm, which was applicable across the different microarray platforms of this study, including our human training set. Second, we restricted our analysis to the well-established molecular MB subtypes. However,

A

Dataset	Platform	Medulloblastoma Subgroups				Normal Human Cerebellum	Samples
		SHH	WNT	Group3	Group4		
GSE37382	P1	51	-	46	188	13	298
GSE30074	P2	9	2	6	13	-	30
GSE41842	P2	3	6	2	8	-	19

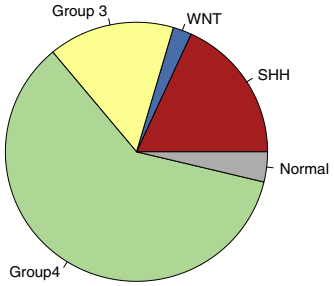

B

Dataset	Platform	Medulloblastoma Subgroups				Normal Human Cerebellum	Samples
		SHH	WNT	Group3	Group4		
GSE37418	P3	10	8	16	39	-	73*
GSE49243	P3	73	-	-	-	-	73
GSE10327	P3	15	9	11	27	-	62
CHO	P4	52	14	51	71	11	199

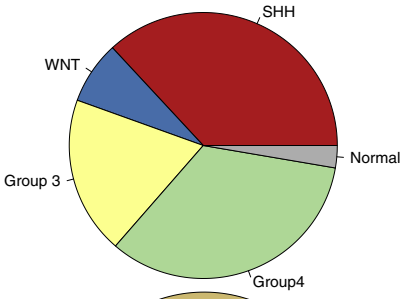

C

Dataset	Platform	Samples
GSE22875	P3	6
GSE7578	P3	3
GSE43552	P3	3
GSE36133	P4	4
E-MTAB-783	P10	6
Cancer Cell Line Encylopedia (CCLE)	P11	4

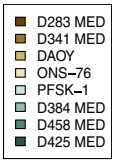

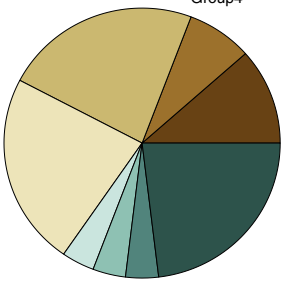

D

Dataset	Platform	Samples
GSE36594	P5	56
GSE24628	P6	16
GSE33199	P6	64
GSE11859	P6	27
GSE50824	P6	19
GSE19534	P6	26
GSE34126	P6	19
GSE2426	P7	14
GSE9299	P8,P9	10
GSE6463	P8,P9	10

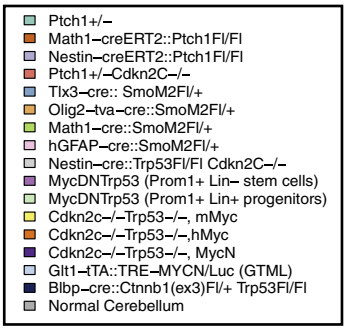

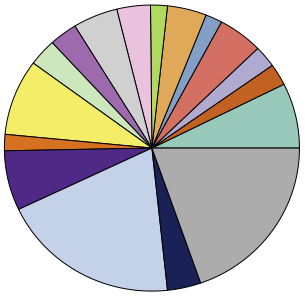

Fig. 6. Overview of MB patients, cell lines, and mouse samples data sets used in this study. Human patient data sets used for MM2S training (I) and testing (II) sets are shown, along a summarized distribution of MB subtypes for each set. The original data set in GSE37418 (*) contains 76 samples, but three samples have been excluded due to their classification as SHH outliers, or unclassified (GSM918628, GSM918618, GSM918644). We collected 26 cell line samples representing 8 common MB cell lines (III). Murine data sets and the corresponding mouse models they represent are also indicated (IV). The gene expression platform and number of samples used for each data set is shown. Gene expression platforms are represented as follows: (P1) Affymetrix Human Gene 1.1 ST, (P2) Affymetrix Human Gene 1.0 ST, (P3) Affymetrix Human Genome U133 Plus 2, (P4) HT Human Genome U133, (P5) Affymetrix Mouse Exon 1.0 ST, (P6) Affymetrix Mouse Genome 430 v2, (P7) Affymetrix Muring Genome U74A v2, (P8) Affymetrix Mouse Expression 430A Array, (P9) Affymetrix Mouse Expression 430B Array, (P10) Affymetrix GeneChip HT human U133A HT_HG-U133A, and (P11) RNA-seq.

the flexibility of our approach enables efficient adaptation of our classifier to alternative subtyping scheme, would another standard be accepted in the field. Finally, while we have tested MM2S extensibility towards prediction of human MB cell lines, the limited number of available cell lines currently available prevents derivation of a consensus subtype for a give cell line. However, it is expected that a clearer subtype classification for these cell lines can be achieved with increased availability of cell line gene expression profiles for MB.

In conclusion, MM2S is the first precedent of a single-sample, multi-system, medulloblastoma-specific classifier. Our ability to effectively characterize both human and mouse MB samples into molecular subtypes addresses the crucial link between translating experimental research conducted on MB model systems to their human MB counterparts. *MM2S* therefore serves to narrow the gap between MB subtype classification methods and the development of singular, subtype-specific diagnosis of human MB patients.

4. Materials and methods

4.1. Human expression array processing and data analysis

Human expression profiles were obtained from a set of 754 normal and tumor medulloblastoma samples previously published across 7 separate studies, which were generated on 4 different low- and high-density microarray platforms [Fig. 6A, B]. The training set for MM2S classification encompassed 347 samples from three studies deposited in the Gene Expression Omnibus (GSE37382, GSE30074, GSE41842; Fig. 6A). These studies were generated using the high-density Gene 1.1 and 1.0 ST arrays, recently developed to supersede standard 3' based microarray platforms [Fig. 6A]. The training set encompass all four MB subtypes (SHH, WNT, Group 3, and Group 4), as well as samples obtained from normal human cerebellum.

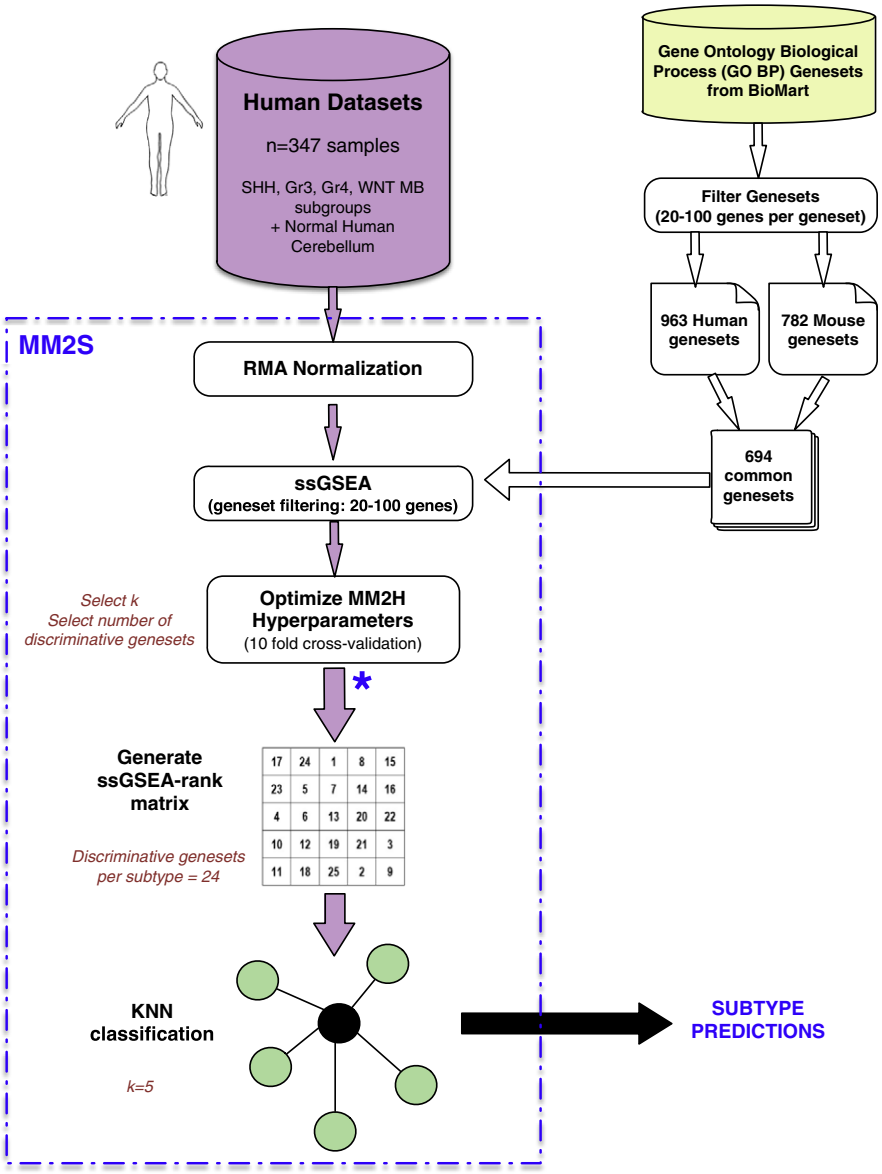

Fig. 7. Overview of MM2S classifier and study design. Overview of the analysis design of the MM2S classifier, which was trained on the 347 human samples across three data sets. MM2S design (depicted by the dotted blue box) accepts gene expression data as input and produces predictions of human subtypes, for each sample, as output.

MM2S efficacy was tested on 407 human gene expression samples spanning 4 separate data sets, including data sets deposited in the Gene Expression Omnibus as well as an additional repository of MB human expression profiles from Cho et al. [3] (abbreviated as CHO data set) [Fig. 6B]. All data sets contain samples across the 4 MB subtypes, except for GSE49243 that only contains SHH samples. The CHO data set is the only set containing normal cerebellum in addition to tumor samples. All the expression profiles for the testing set were generated on the lower density Affymetrix microarray platforms as opposed to Gene ST arrays.

Each data set was processed separately within R/Bioconductor using the *affy* package. A modified *affy* package (version 1.4.0) that could read different microarray platforms was downloaded from BrainArray [17]. CEL files were read using the *ReadAffy* function, and Affymetrix GeneChip probe level data was matched to EntrezGene ID using ENTREZG Custom CDFs (Version 18.0.0) downloaded from BrainArray [17]. CEL files were analyzed using RMA background correction [18] and quantile normalization as part of the *expresso* function. Subtype classifications for all samples for each of the GEO data sets were obtained using the GEOquery package (version 2.30.1).

Survival data pertaining MB patients were extracted for the CHO [3] and GSE37418 [3] data sets. Overall survival curves for both MM2S subtype predictions and original MB subtype classifications were estimated using the Kaplan–Meier estimator and compared using the two-sided log-rank test as implemented in the R/Bioconductor *survcomp* package [19], version 1.14.0; the lower the estimate, the better the prognostic value.

4.2. Cell line expression array processing and data analysis

A total of 26 expression profiles representing 8 human MB cell lines were selected from 6 data sets previously deposited in the Gene Expression Omnibus, Array Express, as well the Cancer Cell Line Encycolpedia (CCLE) [Fig. 6(C)]. Cell lines gene expression profiles obtained from GEO and Array Express were processed similar to the above. For CCLE cell lines profiled using the Illumina RNA-seq platform, BAM files were obtained from CGHub (https://browser.cghub.ucsc.edu/) and processed using Cufflinks (Version 2.2.1) [20] to obtain gene FPKM values.

4.3. Mouse expression array processing and data analysis

A total of 261 mouse expression profiles encompassing over 20 mouse models were selected for medulloblastoma subtype classification [Fig. 6(D)]. These models were obtained from 10 data sets previously deposited in the Gene Expression Omnibus that were generated on 5 separate microarray platforms. All CEL files were processed similar to human patient tumor samples.

4.4. Development of the MM2S classifier

Human and mouse GMT files for Gene Set Enrichment Analysis (GSEA) were generated by extracting gene sets of Gene Ontology Biological Processes (GO BP) from the BioMart database using the R/Bioconductor *biomaRt* package (version 2.18.0) [21,22], and selecting for the "hsapiens_gene_ensembl" and the "mmusculus_gene_ensembl" under the Ensembl biomart repository. Gene sets generated for each species were filtered to include only those with gene set sizes between 20 and 100 genes. A total of 963 and 782 gene sets were generated for human and mouse, respectively. Of these, 694 common gene sets between human and mouse were used to generate the final species-specific GMT files for input into the GSEA.

A single-sample Gene Set Enrichment Analysis (ssGSEA) [23] was conducted on mouse and human expression profiles using the R/Bioconductor GSVA package (version 1.13.1) [24] to obtain single-sample, gene-set enrichment scores (ES). Resultant gene sets were filtered to include gene set sizes containing between 20 and 100 genes. These gene sets were subsequently filtered to select the most discriminative set of subtype-specific gene sets (see next section). The selected gene sets were then combined to generate a ranking matrix, by ranking the gene sets in descending order of their ES scores for each sample, thus producing an ssGSEA-ranked matrix [Fig. 7].

To enable robust classification of the samples into their human medulloblastoma counterparts, we developed a *k*-nearest neighbor (KNN) classification model that uses the Manhattan distance [25] computed from the ssGSEA-rank matrices to make subtype predictions. The accuracy of the classifier was determined using the Matthews Correlation Coefficient (MCC; [26]) on the human training set. Predictions were performed by majority voting of the *k* nearest neighbors. For a given sample, predictions with high confidence (≥80% of votes, that is the proportion of neighbors of the most frequent subtype) are considered indicative of a human subtype, while predictions with <80% confidence are considered to belong to an intermediate subtype.

4.5. Optimization of MM2S hyperparamaters

To optimize our MM2S classifier, two parameters, which are the number of subtype-specific discriminative gene sets, and the number of neighbors (k), must be tuned based on the training set [Fig. 7]. To do so, we performed multiple 10-fold cross validations on the 347 human samples (training data set) to identify the number of neighbors, and the number and identity of discriminative gene sets that yield to the classifier with the best MCC. The 10-fold cross validation was performed 100 times with varying random seeds for patients ordering.

Below we describe how the 10-fold cross validation is conducted within a particular implementation run. Briefly, the KNN classifier was trained on 90% ($n = 312$ samples) of the training set and the remaining 10% ($n = 35$ samples) were used for testing. This procedure was repeated 10 times with non-overlapping testing samples such that each sample is used as part of the testing set once and only once. At each fold of the cross-validation procedure, the MCC score was calculated for k ranging from 1 to 25, and for varying number of gene sets per human MB subtype between 1 and 25. For each human MB subtype, the gene sets were ranked based on the significance of their ES to discriminate the given subtype over all the others combined (SHH vs. Group 3 + Group 4 + WNT + normal for instance), as estimated using the Wilcoxon rank sum test [27]. The selected gene sets were then combined to generate a ranking matrix, for both human and mouse samples, by ranking the gene sets in descending order of their ES scores for each sample. The ssGSEA-ranked matrices were subsequently used as input into the MM2S classifier.

The best k and gene set count used in MM2S were determined by selecting for the paired k and gene set count with the highest average MCC score across the 10 folds, across the 100 implementations of this procedure [S5: Table S5 and S6: Fig. S1].

4.6. Application of MM2S onto human and mouse Cohorts

MM2S has been developed by solely training on the human data set ($n = 347$ samples). To generate robust predictions, and taking into account platform differences for each data set analyzed, we introduced an additional step within MM2S to select for gene sets that are common to human MB and the testing data set (whether human or mouse) before generating ssGSEA-ranked matrices for predictions. For testing mouse data sets for example, ssGSEA-ranked matrices are generated for gene sets that are common to human MB and mouse MB using human and mouse GMT files [Fig. 7]. For a given sample, predictions with high confidence (≥80%) are considered indicative of a corresponding human subtype, while predictions with <80% confidence are considered to belong to an intermediate subtype. Specifically for mouse samples, each sample can be unambiguously classified into its corresponding human subtype by obtaining a consensus prediction across all high confidence predictions for all sample replicates of a particular model.

Authors' contributions

DMAG and BHK conceived and designed the project. DMAG performed the experiments and analyzed the data. PS and DMAG developed the MM2S web server. DMAG, ML, and BHK interpreted the results. DMAG, ML, and BHK wrote the manuscript. All authors read and approved the final manuscript.

Supplementary data to this article can be found online at http://dx.doi.org/10.1016/j.ygeno.2015.05.002.

Acknowledgments

DMAG is supported by a CIBC-Brain Canada Brain Cancer Research Training Award. BHK was supported by the Gattuso Slaight Personalized Cancer Medicine Fund at Princess Margaret Cancer Centre and the Cancer Research Society. The authors would like to thank Robert Castelo and Justin Guinney for their help and updates to the GSVA package. The authors also thank Vijay Ramaswamy, Marc Remke, and Michael Taylor for their discussions and feedback on different aspects of this study.

References

[1] M.C. Thompson, C. Fuller, T.L. Hogg, J. Dalton, D. Finkelstein, C.C. Lau, M. Chintagumpala, A. Adesina, D.M. Ashley, S.J. Kellie, M.D. Taylor, T. Curran, A. Gajjar, R.J. Gilbertson, Genomics identifies medulloblastoma subgroups that are enriched for specific genetic alterations, J. Clin. Oncol. 24 (2006) 1924–1931.

[2] M. Kool, J. Koster, J. Bunt, N.E. Hasselt, A. Lakeman, P. van Sluis, D. Troost, N.S. Meeteren, H.N. Caron, J. Cloos, A. Mrsic, B. Ylstra, W. Grajkowska, W. Hartmann, T. Pietsch, D. Ellison, S.C. Clifford, R. Versteeg, Integrated genomics identifies five medulloblastoma subtypes with distinct genetic profiles, pathway signatures and clinicopathological features, PLoS One 3 (2008) e3088.

[3] Y.J. Cho, A. Tsherniak, P. Tamayo, S. Santagata, A. Ligon, H. Greulich, R. Berhoukim, V. Amani, L. Goumnerova, C.G. Eberhart, C.C. Lau, J.M. Olson, R.J. Gilbertson, A. Gajjar, O. Delattre, M. Kool, K. Ligon, M. Meyerson, J.P. Mesirov, S.L. Pomeroy, Integrative genomic analysis of medulloblastoma identifies a molecular subgroup that drives poor clinical outcome, J. Clin. Oncol. 29 (2011) 1424–1430.

[4] P.A. Northcott, A. Korshunov, H. Witt, T. Hielscher, C.G. Eberhart, S. Mack, E. Bouffet, S.C. Clifford, C.E. Hawkins, P. French, J.T. Rutka, S. Pfister, M.D. Taylor, Medulloblastoma comprises four distinct molecular variants, J. Clin. Oncol. 29 (2011) 1408–1414.

[5] M.D. Taylor, P.A. Northcott, A. Korshunov, M. Remke, Y.J. Cho, S.C. Clifford, C.G. Eberhart, D.W. Parsons, S. Rutkowski, A. Gajjar, D.W. Ellison, P. Lichter, R.J. Gilbertson, S.L. Pomeroy, M. Kool, S.M. Pfister, Molecular subgroups of medulloblastoma: the current consensus, Acta Neuropathol. 123 (2012) 465–472.
[6] M. Kool, A. Korshunov, M. Remke, D.T. Jones, M. Schlanstein, P.A. Northcott, Y.J. Cho, J. Koster, A. Schouten-van Meeteren, D. van Vuurden, S.C. Clifford, T. Pietsch, A.O. von Bueren, S. Rutkowski, M. McCabe, V.P. Collins, M.L. Backlund, C. Haberler, F. Bourdeaut, O. Delattre, F. Doz, D.W. Ellison, R.J. Gilbertson, S.L. Pomeroy, M.D. Taylor, P. Lichter, S.M. Pfister, Molecular subgroups of medulloblastoma: an international meta-analysis of transcriptome, genetic aberrations, and clinical data of WNT, SHH, Group 3, and Group 4 medulloblastomas, Acta Neuropathol. 123 (2012) 473–484.
[7] D.T. Jones, N. Jager, M. Kool, T. Zichner, B. Hutter, M. Sultan, Y.J. Cho, T.J. Pugh, V. Hovestadt, A.M. Stutz, T. Rausch, H.J. Warnatz, M. Ryzhova, S. Bender, D. Sturm, S. Pleier, H. Cin, E. Pfaff, L. Sieber, A. Wittmann, M. Remke, H. Witt, S. Hutter, T. Tzaridis, J. Weischenfeldt, B. Raeder, M. Avci, V. Amstislavskiy, M. Zapatka, U.D. Weber, Q. Wang, B. Lasitschka, C.C. Bartholomae, M. Schmidt, C. von Kalle, V. Ast, C. Lawerenz, J. Eils, R. Kabbe, V. Benes, P. van Sluis, J. Koster, R. Volckmann, D. Shih, M.J. Betts, R.B. Russell, S. Coco, G.P. Tonini, U. Schuller, V. Hans, N. Graf, Y.J. Kim, C. Monoranu, W. Roggendorf, A. Unterberg, C. Herold-Mende, T. Milde, A.E. Kulozik, A. von Deimling, O. Witt, E. Maass, J. Rossler, M. Ebinger, M.U. Schuhmann, M.C. Fruhwald, M. Hasselblatt, N. Jabado, S. Rutkowski, A.O. von Bueren, D. Williamson, S.C. Clifford, M.G. McCabe, V.P. Collins, S. Wolf, S. Wiemann, H. Lehrach, B. Brors, W. Scheurlen, J. Felsberg, G. Reifenberger, P.A. Northcott, M.D. Taylor, M. Meyerson, S.L. Pomeroy, M.L. Yaspo, J.O. Korbel, A. Korshunov, R. Eils, S.M. Pfister, P. Lichter, Dissecting the genomic complexity underlying medulloblastoma, Nature 488 (2012) 100–105.
[8] G. Robinson, M. Parker, T.A. Kranenburg, C. Lu, X. Chen, L. Ding, T.N. Phoenix, E. Hedlund, L. Wei, X. Zhu, N. Chalhoub, S.J. Baker, R. Huether, R. Kriwacki, N. Curley, R. Thiruvenkatam, J. Wang, G. Wu, M. Rusch, X. Hong, J. Becksfort, P. Gupta, J. Ma, J. Easton, B. Vadodaria, A. Onar-Thomas, T. Lin, S. Li, S. Pounds, S. Paugh, D. Zhao, D. Kawauchi, M.F. Roussel, D. Finkelstein, D.W. Ellison, C.C. Lau, E. Bouffet, T. Hassall, S. Gururangan, R. Cohn, R.S. Fulton, L.L. Fulton, D.J. Dooling, K. Ochoa, A. Gajjar, E.R. Mardis, R.K. Wilson, J.R. Downing, J. Zhang, R.J. Gilbertson, Novel mutations target distinct subgroups of medulloblastoma, Nature 488 (2012) 43–48.
[9] V. Hovestadt, D.T. Jones, S. Picelli, W. Wang, M. Kool, P.A. Northcott, M. Sultan, K. Stachurski, M. Ryzhova, H.J. Warnatz, M. Ralser, S. Brun, J. Bunt, N. Jager, K. Kleinheinz, S. Erkek, U.D. Weber, C.C. Bartholomae, C. von Kalle, C. Lawerenz, J. Eils, J. Koster, R. Versteeg, T. Milde, O. Witt, S. Schmidt, S. Wolf, T. Pietsch, S. Rutkowski, W. Scheurlen, M.D. Taylor, B. Brors, J. Felsberg, G. Reifenberger, A. Borkhardt, H. Lehrach, R.J. Wechsler-Reya, R. Eils, M.L. Yaspo, P. Landgraf, A. Korshunov, M. Zapatka, B. Radlwimmer, S.M. Pfister, P. Lichter, Decoding the regulatory landscape of medulloblastoma using DNA methylation sequencing, Nature 510 (2014) 537–541.
[10] E.C. Schwalbe, J.C. Lindsey, D. Straughton, T.L. Hogg, M. Cole, H. Megahed, S.L. Ryan, M.E. Lusher, M.D. Taylor, R.J. Gilbertson, D.W. Ellison, S. Bailey, S.C. Clifford, Rapid diagnosis of medulloblastoma molecular subgroups, Clin. Cancer Res. 17 (2011) 1883–1894.
[11] P.A. Northcott, D.J. Shih, M. Remke, Y.J. Cho, M. Kool, C. Hawkins, C.G. Eberhart, A. Dubuc, T. Guettouche, Y. Cardentey, E. Bouffet, S.L. Pomeroy, M. Marra, D. Malkin, J.T. Rutka, A. Korshunov, S. Pfister, M.D. Taylor, Rapid, reliable, and reproducible molecular sub-grouping of clinical medulloblastoma samples, Acta Neuropathol. 123 (2012) 615–626.
[12] S.L. Markant, R.J. Wechsler-Reya, Review: personalized mice: modelling the molecular heterogeneity of medulloblastoma, Neuropathol. Appl. Neurobiol. 38 (2012) 228–240.
[13] S. Pounds, C.L. Gao, R.A. Johnson, K.D. Wright, H. Poppleton, D. Finkelstein, S.E. Leary, R.J. Gilbertson, A procedure to statistically evaluate agreement of differential expression for cross-species genomics, Bioinformatics 27 (2011) 2098–2103.
[14] P. Gibson, Y. Tong, G. Robinson, M.C. Thompson, D.S. Currle, C. Eden, T.A. Kranenburg, T. Hogg, H. Poppleton, J. Martin, D. Finkelstein, S. Pounds, A. Weiss, Z. Patay, M. Scoggins, R. Ogg, Y. Pei, Z.J. Yang, S. Brun, Y. Lee, F. Zindy, J.C. Lindsey, M.M. Taketo, F.A. Boop, R.A. Sanford, A. Gajjar, S.C. Clifford, M.F. Roussel, P.J. McKinnon, D.H. Gutmann, D.W. Ellison, R. Wechsler-Reya, R.J. Gilbertson, Subtypes of medulloblastoma have distinct developmental origins, Nature 468 (2010) 1095–1099.
[15] J. Poschl, S. Stark, P. Neumann, S. Grobner, D. Kawauchi, D.T. Jones, P.A. Northcott, P. Lichter, S.M. Pfister, M. Kool, U. Schuller, Genomic and transcriptomic analyses match medulloblastoma mouse models to their human counterparts, Acta Neuropathol. 128 (2014) 123–136.
[16] J. Mao, K.L. Ligon, E.Y. Rakhlin, S.P. Thayer, R.T. Bronson, D. Rowitch, A.P. McMahon, A novel somatic mouse model to survey tumorigenic potential applied to the Hedgehog pathway, Cancer Res. 66 (2006) 10171–10178.
[17] M. Dai, P. Wang, A.D. Boyd, G. Kostov, B. Athey, E.G. Jones, W.E. Bunney, R.M. Myers, T.P. Speed, H. Akil, S.J. Watson, F. Meng, Evolving gene/transcript definitions significantly alter the interpretation of GeneChip data, Nucleic Acids Res. 33 (2005) e175.
[18] R.A. Irizarry, B.M. Bolstad, F. Collin, L.M. Cope, B. Hobbs, T.P. Speed, Summaries of Affymetrix GeneChip probe level data, Nucleic Acids Res. 31 (2003) e15.
[19] M.S. Schroder, A.C. Culhane, J. Quackenbush, B. Haibe-Kains, survcomp: an R/Bioconductor package for performance assessment and comparison of survival models, Bioinformatics 27 (2011) 3206–3208.
[20] C. Trapnell, A. Roberts, L. Goff, G. Pertea, D. Kim, D.R. Kelley, H. Pimentel, S.L. Salzberg, J.L. Rinn, L. Pachter, Differential gene and transcript expression analysis of RNA-seq experiments with TopHat and Cufflinks, Nat. Protoc. 7 (2012) 562–578.
[21] S. Durinck, Y. Moreau, A. Kasprzyk, S. Davis, B. De Moor, A. Brazma, W. Huber, BioMart and Bioconductor: a powerful link between biological databases and microarray data analysis, Bioinformatics 21 (2005) 3439–3440.
[22] S. Durinck, P.T. Spellman, E. Birney, W. Huber, Mapping identifiers for the integration of genomic datasets with the R/Bioconductor package biomaRt, Nat. Protoc. 4 (2009) 1184–1191.
[23] D.A. Barbie, P. Tamayo, J.S. Boehm, S.Y. Kim, S.E. Moody, I.F. Dunn, A.C. Schinzel, P. Sandy, E. Meylan, C. Scholl, S. Frohling, E.M. Chan, M.L. Sos, K. Michel, C. Mermel, S.J. Silver, B.A. Weir, J.H. Reiling, Q. Sheng, P.B. Gupta, R.C. Wadlow, H. Le, S. Hoersch, B.S. Wittner, S. Ramaswamy, D.M. Livingston, D.M. Sabatini, M. Meyerson, R.K. Thomas, E.S. Lander, J.P. Mesirov, D.E. Root, D.G. Gilliland, T. Jacks, W.C. Hahn, Systematic RNA interference reveals that oncogenic KRAS-driven cancers require TBK1, Nature 462 (2009) 108–112.
[24] S. Hanzelmann, R. Castelo, J. Guinney, GSVA: gene set variation analysis for microarray and RNA-seq data, BMC Bioinformatics 14 (2013) 7.
[25] E.F. Krause, Taxicab Geometry: an adventure in non-Euclidean geometry, Dover Publications, New York, 1987.
[26] B.W. Matthews, Comparison of the predicted and observed secondary structure of T4 phage lysozyme, Biochim. Biophys. Acta 405 (1975) 442–451.
[27] F. Wilcoxon, S.K. Katti, R.A. Wilcox, Critical values and probability levels for the Wilcoxon rank sum test and the Wilcoxon signed rank test/[by], American Cyanamid, Pearl River, N.Y., 1963.